https://doi.org/10.15407/ujpe66.8.684

HAMID AL-JIBBOURI

College of Science, University of Al-Qadisiyah
(Al-Diwaniya 58002, Iraq; e-mail: hamid.aljibbouri@qu.edu.iq)

VARIATIONAL CALCULATION OF LITHIUM-LIKE IONS FROM B^{+2} TO N^{+4} USING β-TYPE ROOTHAAN–HARTREE–FOCK WAVEFUNCTION

Within the KαKβ, KαLα, and KβLα shells in the position space, the properties of a series of three-electron systems, for instance, B^{+2}, C^{+3}, and N^{+4} ions, have been studied. This required the partitioning of the two-particle space-spin density and was explicit for the Hartree–Fock description which have been proposed by considering a basis set based on single-zeta β-type orbitals (βTOs). The one- and two-body radial electronic densities $R(r_1)$, $R(r_1, r_2)$, moments $\langle r_1^n \rangle$, X-ray form factor $\mathcal{F}(s)$, nucleus density $R(0)$, nuclear magnetic shielding constant σ_d, and the diamagnetic susceptibility δ_s in the position space are reported. Our results are realized via the Mathematica program and compared with previous theoretical values in the literature.

Keywords: Roothaan–Hartree–Fock, β-type orbitals, X-ray form factor, nuclear magnetic shielding constant, diamagnetic susceptibility.

1. Introduction

The non-relativistic ground states of three-particle systems have been a topic of the wide quantum computational research using the Roothaan–Hartree–Fock (RHF), configuration-interaction (CI), and Hylleraas wavefunctions [1–4]. The RHF approximation is of crucial importance for the accuracy of results in the estimation of fundamental physical properties of atoms and molecules. Indeed, several kinds of exponential-type orbital (ETO), for instance, Slater-type orbitals (STOs) [5–7] and β-type orbitals (βTOs) [8] have already discussed and realized in the calculations of the electronic structure of atoms and molecules. However, STOs can be represented by linear combinations of the β function [9–11]. The major feature of the β function is its very simple Fourier transform [12] which is related to compact general formulas for molecular integrals derivable using the Fourier transform method [13]. Various studies of three-electron systems, for instance, in Refs. [14, 15] present the nonrelativistic variational calculation of Li-isoelectronic series using the Hylleraas functions. The radial properties of the electronic density function in Refs. [16, 17] have been studied in closed form for the ^{2}S states. The density at nuclei expectation values, as well as quadrupole and octupole polarizabilities, have been considered in Refs. [18–20], respectively. In Ref. [21], the scattering and magnetic form factors were calculated, respectively, for the ground states of Li-like ions obtained via highly accurate configuration-interaction wave function. Indeed, the scattering form factors have studied in Refs. [22, 23] for the ground states of the Li-like ions with the full core plus correlation wave function.

Motivated by this, we carried out the HF wavefunction calculations for KαKβ, KαLα, and KβLα shells of three-electron systems that possess the basis sets described by single-zeta βTOs [8]. We mainly focus on the theoretical technique for one- and two-radial densities $R(r_1)$ and $R(r_1, r_2)$, respectively, which have

an important feature in the realization in the atomic and molecular studies [24, 25] and determine the radial expectation moments $\langle r_1^n \rangle$ for $n = -2, ..., 2$, electron density at a nucleus $R(0)$, X-ray form factor $\mathcal{F}(s)$, nuclear magnetic shielding constant σ_d, and the diamagnetic susceptibility δ_s.

2. Wavefunction

The trial wavefunction of the RHF approximation is considered to be a Slater determinant of mutually orthonormal single-particle states, and it satisfies the antisymmetry with respect to the interchange of any two particles[26]. We have

$$\Psi_{HF}(\mathbf{x}_1, \mathbf{x}_2, ..., \mathbf{x}_N) = \\ = \frac{1}{\sqrt{N!}} \begin{vmatrix} \chi_1(\mathbf{x}_1) & \chi_2(\mathbf{x}_1) & ... & \chi_N(\mathbf{x}_1) \\ \chi_1(\mathbf{x}_2) & \chi_2(\mathbf{x}_2) & ... & \chi_N(\mathbf{x}_2) \\ \vdots & \vdots & & \vdots \\ \chi_1(\mathbf{x}_N) & \chi_2(\mathbf{x}_N) & ... & \chi_N(\mathbf{x}_N) \end{vmatrix}. \quad (1)$$

Here, $\chi(\mathbf{x}_i)$ denote the spin-orbital components and is defined as

$$\chi = \sum_{i=1}^{j} C_{nlm}^i \varphi_{nlm}, \quad (2)$$

where C_{nlm}^i is the constant coefficient that is calculated by minimizing the total energy, and the basis function φ_{nlm} denotes the normalized βTOs which take the form

$$\chi_{q,l}^m(\alpha; r, \theta, \varphi) = N_{q,l}\, r^l Y_l^m(\theta, \Phi)\, R_{q-1/2}(\alpha r) \quad (3)$$

where $N_{q,l}$ means the normalization of the radial part [9, 11, 27, 28]:

$$N_{q,l} = \frac{2^{l+q}\alpha^{l+1}}{(l+q)!}\sqrt{\frac{\alpha\Gamma(2l+2q+2)\, l!\Gamma(l+2q)}{\Gamma(2l+4q)\,\Gamma(2l+1)}}, \quad (4)$$

where $\Gamma(x)$ is the gamma function; $Y_l^m(\theta, \Phi)$ denotes the complex or real spherical harmonic:

$$Y_l^m(\theta, \Phi) = \frac{1}{\sqrt{2\pi}} P_{l|m|}(\cos\theta)\, e^{im\Phi}. \quad (5)$$

Here, $P_{l|m|}$ are normalized associated Legendre functions for complex spherical harmonics. For real harmonics, $\Phi_m(\Phi)$ has the form

$$\Phi_m(\Phi) = \frac{1}{\sqrt{\pi(1+\delta_{m0})}} \begin{cases} \cos|m|\,\Phi, & \text{for } m \geq 0, \\ \sin|m|\,\Phi, & \text{for } m < 0, \end{cases} \quad (6)$$

$R_{q-1/2}(\alpha r)$ represents the reduced Bessel function with integer $q \geq 1$ and is given by

$$R_{q-1/2}(\alpha r) = e^{-\alpha r} \sum_{i=0}^{q-1} \frac{\Gamma(q+i)(\alpha r)^{q-i-1}}{\Gamma(q-i)\, i! 2^i}. \quad (7)$$

We will show that βTOs have form of a linear combination of STOs [8, 9] due to the simplicity of their Fourier transforms. This enables us to approximate two-center distributions by a sum of one-center distributions placed at the line connecting the original two centers [8, 29]. Therefore, we have considered the single Zeta βTOs basis sets that were obtained in Ref. [8].

3. Theoretical Consideration

3.1. Two-Radial Density Function $R(r_1, r_2)$

The two-electron density function $\Pi(x_1, x_2)$ denotes the probability density of the electrons, whereas the position of one electron at r_1, while the other electron at r_2 simultaneously, $\Pi(x_1, x_2)$ is defined by [30, 31]

$$\Pi(\mathbf{x}_1, \mathbf{x}_2) = \mathcal{N} \int d\mathbf{x}_p ... d\mathbf{x}_q \Psi(\mathbf{x}_1, \mathbf{x_2}, \mathbf{x}_p, ..., \mathbf{x}_q) \times \\ \times \Psi^*(\mathbf{x}_1, \mathbf{x_2}, \mathbf{x}_p, ..., \mathbf{x}_q), \quad (8)$$

where $\mathbf{x}_i = (r_i, \Theta_i, \Phi_i, \gamma_i)$ represents the combination of space and spin coordinates of N electrons, while $d\mathbf{x}_p ... d\mathbf{x}_q$ correspond to the integration over all N electrons except for 1 and 2. In particular, the constant $\mathcal{N} = \int \Pi(x_1, x_2) dx_1 dx_2 = N!/(2!(N-2)!)$ is the normalization one for electron pairs in the system. The three-electron systems have three pairs, and the total electron density function can be written as $\Pi_{\text{HF}}(r_1, r_2) = \Pi_{\text{K}}^{\alpha\beta}(r_1, r_2) + \Pi_{\text{KL}}^{\beta\alpha}(r_1, r_2) + \Pi_{\text{KL}}^{\alpha\alpha}(r_1, r_2)$. Let us now illustrate the concept of density functions through a consideration of the three lowest electronic states of the three-electron ions after the integration over all spins and angular functions. This yields

$$\begin{aligned} &\Pi_{\text{K}}^{\alpha\beta}(r_1, r_2) = \chi_{1s}^2(r_1)\chi_{1s}^2(r_2), \\ &\Pi_{\text{KL}}^{\beta\alpha}(r_1, r_2) = \frac{1}{2}(\chi_{1s}^2(r_1)\chi_{2s}^2(r_2) + \chi_{2s}^2(r_1)\chi_{1s}^2(r_2)), \\ &\Pi_{\text{KL}}^{\alpha\alpha}(r_1, r_2) = \frac{1}{2}(\chi_{1s}^2(r_1)\chi_{2s}^2(r_2) + \chi_{2s}^2(r_1)\chi_{1s}^2(r_2) - \\ &- 2\chi_{1s}(r_1)\chi_{2s}(r_1)\chi_{1s}(r_2)\chi_{2s}(r_2)). \end{aligned} \quad (9)$$

The two-particle radial density $R(r_1, r_2)$ is the probability of that two electrons are located on a radius

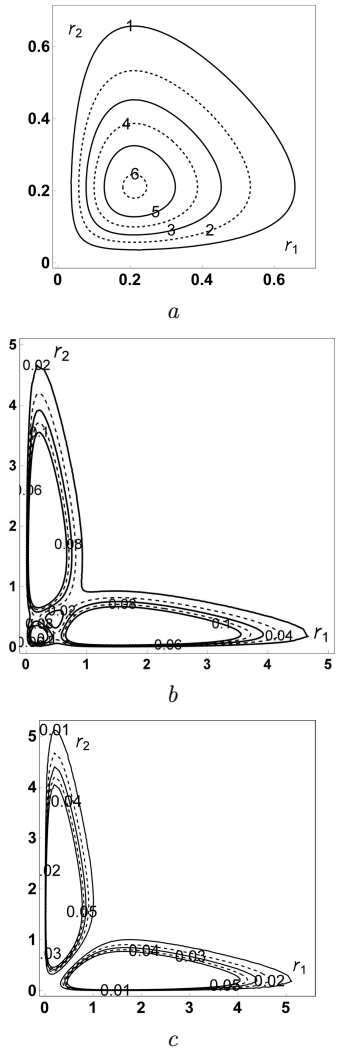

Fig. 1. Contour diagram of the radial two-density function $R(r_1, r_2)$. Eq. (10) for B^{+2} ion in atomic units (a.u.): the ground state of $R_K^{\alpha\beta}(r_1, r_2)$ has maxima $R_K^{\alpha\beta}(r_1, r_2) = 6.14435$ located at $r_1 = r_2 = 0.210976a_0$ (a); $R_{KL}^{\beta\alpha}(r_1, r_2)$ has three maxima $R_K^{\beta\alpha}(r_1, r_2) = 0.207$ located at $r_1 = r_2 = 0.18a_0$, $R_K^{\beta\alpha}(r_1, r_2) = 0.664$ located at $r_1 = 0.210, r_2 = 1.52a_0$, and $R_K^{1}(r_1, r_2) = 0.664$ located at $r_1 = 1.523, r_2 = 0.210a_0$ (b); and $R_{KL}^{\alpha\alpha}(r_1, r_2)$ has two maxima $R_K^{\alpha\alpha}(r_1, r_2) = 0.677$ located at $r_1 = 0.210, r_2 = 1.492a_0$ and $R_K^{\alpha\alpha}(r_1, r_2) = 0.677$ located at $r_1 = 1.492, r_2 = 0.210a_0$ (c)

at r_1 and r_2, respectively:

$$R_K^{\alpha\beta}(r_1, r_2) = r_1^2 r_2^2 \chi_{1s}^2(r_1)\chi_{1s}^2(r_2),$$

$$R_{KL}^{\beta\alpha}(r_1, r_2) = \frac{r_1^2 r_2^2}{2}(\chi_{1s}^2(r_1)\chi_{2s}^2(r_2) + \chi_{2s}^2(r_1)\chi_{1s}^2(r_2)),$$

$$R_{KL}^{\alpha\alpha}(r_1, r_2) = \frac{r_1^2 r_2^2}{2}(\chi_{1s}^2(r_1)\chi_{2s}^2(r_2) + \chi_{2s}^2(r_1)\chi_{1s}^2(r_2) - 2\chi_{1s}(r_1)\chi_{2s}(r_1)\chi_{1s}(r_2)\chi_{2s}(r_2)). \quad (10)$$

Equations (10) can be evaluated by the analysis of RHF wavefunction based on single Zeta βTOs of the form given in Eqs. (2) and (3).

3.2. One-radial density function $R(r_1)$ and the expectation value $\langle r_1^n \rangle$

The one-radial density function has paved a typical issue for our study. It gives us the idea and characterization of the dynamics of atomic and molecular studies and is the basis of theories of the atomic density function [21–24, 30–32]. The one-radial quantity $R(r_1)$ is the probability of finding the electrons in the whole shell in the interval from r_1 to $r_1 + dr_1$. The radial density function is obtained via the integration of Eqs. (10) with respect to dr_2. We get

$$R(r_1) = \int_0^\infty R(r_1, r_2) dr_2. \quad (11)$$

The expectation value $\langle r_1^n \rangle$ is defined from Eq. (11) as

$$\langle r_1^n \rangle = \int_0^\infty R(r_1)\, r_1^n dr_1. \quad (12)$$

Equation (12) is used to calculate the electron-nuclear potential $V_{en} = -Z\sum_{i=1}^{3}\langle r_i^{-1}\rangle$, were Z denotes the atomic number, and the nuclear magnetic shielding constant $\sigma_d = -\alpha^2/3\sum_{i=1}^{3}\langle r_i^{-1}\rangle$, with the fine structure constant $\alpha = 7.297353 \times 10^{-3}$ a.u. [15]. For $n = 2$, we evaluated the diamagnetic susceptibility $\delta_s = -\alpha^2/6\sum_{i=1}^{3}\langle r_i^2\rangle$ [15]. Some of the expectation values can be related to several oscillator strength sums [15].

3.3. Atomic form factor $\mathcal{F}(s)$

Theoretical atomic form factors $\mathcal{F}(s)$ are utilized to characterize the performance of the scattering of a given atom and the direction, respectively. Indeed, it is evaluated from the Fourier transform of the one-radial density function [15, 33–35]:

$$\mathcal{F}(s) = \int_0^\infty R(r_1)\, j_0(sr_1)\, dr_1, \quad (13)$$

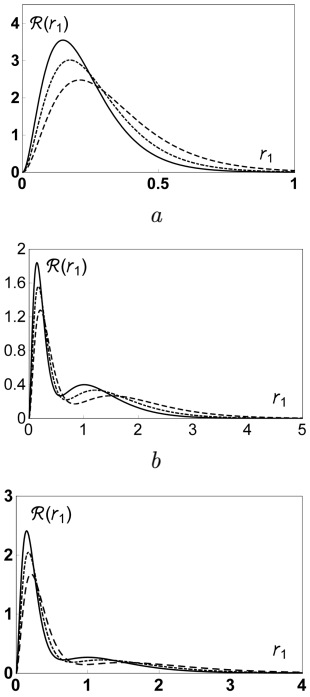

Fig. 2. One-radial density function $R(r_1)$ by Eqs. (11). $R_{\mathrm{K}}^{\alpha\beta}(r_1)$ (*a*), $R_{\mathrm{KL}}^{\beta\alpha}(r_1) = R_{\mathrm{KL}}^{\alpha\alpha}(r_1)$ (*b*), and total $R(r_1)$ (*c*). Dashed, dot-dashed, and solid curves correspond to B^{+2}, C^{+3}, and N^{+4}, respectively

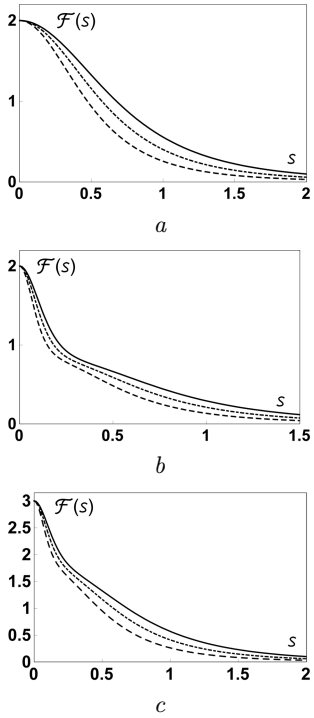

Fig. 3. Scattering form factor $\mathcal{F}(s)$ by Eqs. (13) versus s. $\mathcal{F}_{\mathrm{K}}^{\alpha\beta}(s)$ (*a*), $\mathcal{F}_{\mathrm{KL}}^{\alpha\alpha}(s) = \mathcal{F}_{\mathrm{KL}}^{\beta\alpha}(s)$ (*b*), and total $\mathcal{F}(s)$ (*c*). Dashed, dot-dashed, and solid curves correspond to B^{+2}, C^{+3}, and N^{+4}, respectively

where j_0 is the first-kind spherical Bessel function ($j_0(x) = x^{-1}\sin x$), s is the magnitude of the vector of momentum transfer that depends on the radiation wavelength λ and the scattering angle 2θ according to $s = 4\pi\sin\theta/\lambda$.

4. Results and Discussions

Our results are implemented via the Mathematica Program version (10.1.01). Furthermore, we have studied the ground state B^{+2}, C^{+3}, and N^{+4} ions by using the RHF wavefunction. The basis sets are examined and illustrated by single-zeta βTOs (see Eqs (2) and (3), respectively). Afterward, we have computed $R(r_1, r_2)$, $R(r_1)$, $\langle r_1^n\rangle$, and $\mathcal{F}(s)$, as well as some physical properties.

Figure 1 shows the contour shapes for KαKβ, KαLα, and KβLα shells and the two-radial density function for B^{+2} ion by Eqs. (10). We note that the probability distribution is statically uncorrelated, but it remains correlated in the space-spin configuration space. Due to the antisymmetry condition, the radial two-density functions in Figs. 1, *b* and *c* show different two particle spin-free densities with respect to the coupling of spin and space coordinates.

Furthermore, due to the Fermi heap, the exchange term increases the probability for two electrons to be in the same spatial region (see Fig. 1, *b*), while the exchange term reduces the probability for two electrons to be close to each other (Fermi hole, Fig. 1, *c*).

For the KαKβ, KαLα, and KβLα shells, Fig. 2 shows the one-radial density functions for B^{+2}, C^{+3}, and N^{+4} ions which are obtained via single-Zeta βTOs with the RHF wavefunction. The curves in Fig. 2, *a* show the probability to find an electron at the distance r_1 from the center of the atom. The maxima $R_{\mathrm{K}}^{\alpha\beta}(r_1)$ for B^{+2}, C^{+3}, and N^{+4} are 2.47878, 3.01521, and 3.54955, respectively. For different maximum points, their distances to the nucleus increase with Z due to the attraction force of the nucleus. In Figs. 1, *b*, *c*, the one-radial density functions for individual shells, as well as the total $R(r_1)$, have two maximum points, one of them is related to the probability of finding the electron in the K-shell, while the

The expectation value $\langle r_1^n \rangle$ for different exponent parameters n, the nuclear magnetic shielding constant σ_d, and the diamagnetic susceptibility δ_s in a.u.

Ions	Shells	$\langle r_1^{-2} \rangle$	$\langle r_1^{-1} \rangle$	$\langle r_1^{1} \rangle$	$\langle r_1^{2} \rangle$	$\sigma_d \times 10^{-4}$	$\delta_s \times 10^{-5}$	$R(0)$
B^{+2}	K	44.444	4.668	0.326	0.144	1.657	0.256	34.459
B^{+2}	KL	23.280	2.694	1.147	2.403	0.956	4.266	17.979
C^{+3}	K	65.114	5.660	0.268	0.097	2.009	0.173	60.748
C^{+3}	KL	34.234	3.281	0.926	1.567	1.165	2.781	31.831
N^{+4}	K	89.762	6.651	0.228	0.070	2.361	0.124	97.970
N^{+4}	KL	47.2874	3.866	0.778	1.103	1.372	1.959	51.422

second one determines the probability of finding the electron in the L-shell. In particular, the K-shell has one peak higher than in the L-shell according to the attraction force.

In Fig. 3, we show the scattering form factor given by Eq. (13) for KαKβ, KαLα, and KβLα shells of B^{+2}, C^{+3}, and N^{+4} ions. If the scattering angle is zero, we note that $\mathcal{F}(s)$ depends on the number of electrons in the ion shell. In particular, the total scattering occurs according to the constructive interference of X-rays that are scattered on the electrons and then gradually degenerate, by increasing the scattering angle till to a decline of the minimum value which is different for different shells of atoms or ions.

Figure 3, *a* indicates that, due to the higher attraction force toward the nucleus with respect to other electrons, the values of $\mathcal{F}(s)$ are greater than those for other shells, and $\mathcal{F}(s)$ values decrease, as the path difference of the scattered waves increases. According to the charge distribution at the internal shell, we show in Figs. 3, *b* and 3, it c that $\mathcal{F}(s)$ values having a maximum point will sharply decrease followed by the curvature and then slowly decline. The total atomic scattering factor was calculated in Ref. [21] for the ground state of Li-like ions from $Z = 4$–10 via the configuration interaction framework. Our results show a good agreement with Ref. [21, 35].

Table presents the examination of $\langle r_1^n \rangle$ for different exponent parameters n for KαKβ, KαLα, and KβLα shells for B^{+2}, C^{+3}, and N^{+4} ions. For several Z, the $\langle r_1^n \rangle$ increases, when the exponent n goes from $n = -1$ to $n = -2$ and decreases, when $n = 1$ to $n = 2$ according to the weak attractive force between the nucleus and the electrons in outer shells. Our results have a good agreement with Refs. [5, 6, 8]. The total values of moments $\langle r_1^n \rangle$ for ions determine the average value for different shells in an atom $\langle r_1^n \rangle = \frac{1}{3}\left(\langle r_1^n \rangle_K + 2\langle r_1^n \rangle_{KL}\right)$. The nuclear magnetic shielding constant σ_d increases as the number of electrons increases from 3 to 5 due to the magnetic field proportional directly to the number of electrons, while the diamagnetic susceptibility δ_s decreases, as Z increases. In particular, the nuclear magnetic shielding constant for the K-shell is larger, than for the KL-shell due to the attraction force. The nucleus densities $R(0)$ for B^{+2}, C^{+3}, and N^{+4} ions increase with the atomic number Z. This happens for all shells in each atom in the sequence. Indeed, the nucleus density $R(0)$ for the K-shell is greater, than that for the KL- shell due to the increased distance among the electrons and the nucleus.

5. Conclusions

We have studied the properties of the KαKβ, KαLα, and KβLα shells of B^{+2}, C^{+3}, and N^{+4} ions by considering a basis set based on single-zeta βTOs and the RHF wavefunction which characterize the global properties quite well. The one- and two-body radial electronic densities $R(r_1)$ and $R(r_1, r_2)$ in the position space have been discussed, as well as the expectation values for several moments $\langle r_1^n \rangle$ studied with the use of $R(r_1)$. We have studied some physical properties such as the nucleus density $R(0)$, X-ray form factor $\mathcal{F}(s)$, nuclear magnetic shielding constant, and the diamagnetic susceptibility δ_s that increase (decrease), as Z increases. This provides a valuable reference for other researched subjects in future. Inded, we read off that the full scattering of X-rays occurs at $\theta = 0$, and σ_d increases with the atomic number Z.

I thank Prof. Dr. Khalil Al-Bayati for insightful comments.

1. A. Cooksy. *Physical Chemistry: Quantum Chemistry and Molecular Interactions* (Prentice Hall, 2013).
2. C. Hättig, W. Klopper, A. Köhn, D.P. Tew. Explicitly correlated electrons in molecules. *Chem. Rev.* **112**, 4 (2012).
3. Jason K. Pearson, Peter M. W. Gill, Jesus M. Ugalde, and Russell J. Boyd. Can correlation bring electrons closer together? *Mol. Phys.* **107**, 1089 (2009).
4. G.A. Sekh, B.T.S. Chatterjee. Insights from intracules and Coulomb holes. *Eur. J. Phys.* **41** 45403 (2020).
5. E. Clementi, C. Roetti. Roothaan-Hartree-Fock atomic wavefunctions: Basis functions and their coefficients for ground and certain excited states of neutral and ionized atoms, $Z \leq 54$. *At. Data Nucl. Data Tables* **14**, 177 (1974).
6. C.F. Bunge, J.A. Barrientos, A.V. Bunge, J.A. Cogordan. Hartree-Fock and Roothaan-Hartree-Fock energies for the ground states of He through Xe. *Phys. Rev. A* **46**, 3691 (1992).
7. I.I. Guseinov, E. Sahin, M. Erturk. An improvement on $\psi(\alpha^*)$ exponential type orbitals for atoms in standard convention. *Mol. Phys.* **112**, 35 (2014).
8. I. Ema, J.M. Garcia de la Vega, B. Miguel, J. Dotterweich, H. Meissner, E.O. Steinborn. Expotential-type basis functions: Single- and double-zeta B function basis sets for the ground states of neutral atoms from $Z = 2$ to $Z = 36$. *At. Data Nucl. Data Tables.* **72**, 57 (1999).
9. E. Filter, E.O. Steinborn. Extremely compact formulas for molecular two-center one-electron integrals and Coulomb integrals over Slater-type atomic orbitals. *Phys. Rev. A* **18**, 1 (1978).
10. M. Ertürk, E. Ozturk. Modified B function basis sets with generalized hyperbolic cosine functions. *Comput. Theor. Chem.* **1127**, 37 (2018).
11. M. Ertürk, E. Sahin. Generalized B functions applied to atomic calculations *Chem. Phys.* **529**, 110549 (2020).
12. J. Weniger, E.O. Steinborn. The Fourier transforms of some exponential-type basis functions and their relevance to multicenter problems. *J. Chem. Phys.* **78**, 6121 (1983).
13. J. Weniger, E.O. Steinborn. Numerical properties of the convolution theorems of B functions. *Phys. Rev. A* **28**, 2026 (1983).
14. F.W. King. Calculations on the ^{2}S ground states of some members of the Li isoelectronic series. *Phys. Rev. A* **40**, 1735 (1989).
15. F.W. King. Progress on high precision calculations for the ground state of atomic lithium *J. Mol. Struct. (Theochem)* **400**, 7 (1997).
16. F.W. King, P.R. Dressel. Compact expressions for the radial electronic density functions for the ^{2}S states of three-electron systems *J. Chem. Phys.* **90**, 6449 (1989).
17. Guan Xiao-xu, Wang Zhi-wen. Radial electronic density for the ground state of the lithium isoelectronic sequence. *Chin. Phys. Lett.* **15**, 489 (1998).
18. C. Chen, W. Zhi-Wen. Inequalities of the electron density at the nucleus and radial expectation values of the ground state for the lithium isoelectronic sequence. *Chinese Phys.* **12**, 604 (2003).
19. C. Chen. Studies of the electron density at the nucleus and radial expectation values of the ground state for lithium-like systems from $Z = 11$ to 18. *Eur. Phys. J. D.* **56**, 303 (2010).
20. C. Chen, W. Zhi-Wen. Quadrupole and octupole polarizabilities for the ground states of lithiumlike systems from $Z = 3$ to 20 *J. Chem. Phys.* **121**, 4171 (2004).
21. H. Schmider, R.O. Esquivel, R.P. Sagar, V.H. Smith, Jr. Spin magnetic form factors for lithium and its isoelectronic series in position and momentum space. *J. Phys. B* **26**, 2943 (1993).
22. C. Chen, W. Zhi-Wen. Total atomic scattering factors for the ground states of the lithium isoelectronic sequence from Na^{+8} to Ca^{+17}. *J. Chem. Phys.* **122**, 024305 (2005).
23. C. Chen, W. Zhi-Wen. Total atomic scattering factors of $1s^2 3s^2$S states for lithium isoelectronic sequence. *Commun. Theor. Phys.* **50**, 473 (2008).
24. R. Benesch. Algebraic determination of electron-nuclear and electron-electron distribution functions from Hhller-aas type wavefunctions. *J. Phys. B: At. Mol. Phys.* **4**, 1403 (1971).
25. R.J. Boyd, C. Sarasola, J.M. Ugalde. Intracule densities and electron correlation in the hydrogen molecule *J. Phys. B: At. Mol. Opt. Phys.* **21**, 2555 (1988).
26. P. Atkins, J. De Paula, R.S. Friedman, *Quanta, Matter, and Change. A Molecular Approach to Physical Chemistry* (Oxford University Press, 2009).
27. H. Al-Jibbouri. Ground state of radial-radial distribution function for C^{+4} and O^{+6} ions. *J. Phys. Con. Ser.* **1294**, 052052 (2019).
28. H. Al-Jibbouri, Ammar Alhasan. Study the inter-particle function for some electronic system. *J. Phys. Con. Ser.* **1294**, 022014 (2019).
29. J.F. Rico, R. Lopez, G. Ramirez, I. Ema. Multiple one-center expansions of charge distributions associated with Slater orbitals. *J. Mol. Struct. (Theochem)* **433**, 7 (1998).
30. K.E. Banyard, K.H. Al-Bayati. Intra- and inter-shell correlation effects in Li-like ions: Coulomb holes and their interpretation. *J. Phys. B: At. Mol. Phys.* **19**, 2211 (1986).
31. K.E. Banyard, K.H. Al-Bayati, P.K. Youngman. Coulomb correlation in a doubly occupied K shell: the influence of outer electrons. *J. Phys. B: At. Mol. Opt. Phys.* **22**, 971 (1989).
32. V.A. Volotka, A.D. Glazov, I.I. Tupitsyn, S.N. Oreshkina, G. Plunien, M.V. Shabaev. Ground-state hyperfine structure of H-, Li-, and B-like ions in the intermediate-Z region. *Phys. Rev. A* **78**, 062507 (2008).
33. L.S. Bartell, R.M. Gavin Jr. Effects of electron correlation in X-ray and electron diffraction. II. Influence of nuclear charge in two-electron systems. *J. Chem. Phys.* **43**, 856 (1965).
34. J.H. Hubbell, Wm.J. Veigele t, E.A. Briggs, R.T. Brown, D.T. Cromer, R. J. Howenon. Atomic form factors, incoherent scattering functions, and photon scattering cross sections. *J. Phys. Chern. Ref. Data* **4**, 471 (1975).

35. R.T. Brown. Coherent and incoherent X-ray scattering by bound electrons. II. Three- and four-electron atoms. *Phys. Rev. A* **2**, 614 (1970).

Received 28.08.20

Хемід Ель-Джіббурі

ВАРІАЦІЙНИЙ РОЗРАХУНОК
Li-ПОДІБНИХ ЙОНІВ ВІД B^{+2} ДО N^{+4}
З ВИКОРИСТАННЯМ ХВИЛЬОВОЇ
ФУНКЦІЇ ХАРТРІ–ФОКА–РУТААНА β-ТИПУ

Вивчено властивості низки триелектронних систем в межах просторових оболонок KαKβ, KαLα і KβLα, наприклад, B^{+2}, C^{+3} і N^{+4} йонів. Це вимагало проведення розбиття двочастинкових функцій просторової і спінової густин, що можливо в рамках моделі Хартрі–Фока з базисами, побудованими на $1z$ орбіталях β-типу. Знайдено одно- і двочастинкові радіальні електронні розподіли густини $R(r_1)$ і $R(r_1, r_2)$, моменти $\langle r_1^n \rangle$, формфактори рентгенівського випромінювання $\mathcal{F}(s)$, густину ядра $R(0)$, константу ядерного магнітного екранування σ_d і діамагнітну сприйнятливість δ_s. Результати отримано з використанням програми Mathematica і порівняно з відомими теоретичними даними.

Ключові слова: метод Хартрі–Фока–Рутаана, орбіталі β-типу, формфактор рентгенівського випромінювання, константа ядерного магнітного екранування, діамагнітна сприйнятливість.